

Experimental Stress Analysis

PROCEEDINGS OF THE
8TH INTERNATIONAL CONFERENCE

1986

Experimental Stress Analysis

Proceedings of the VIIIth International Conference on Experimental Stress Analysis, Amsterdam, The Netherlands, May 12–16, 1986

*Organized by: Netherlands Organization for Applied Scientific Research (TNO)
on behalf of The Permanent Committee for Stress Analysis*

edited by

H. WIERINGA

TNO-IWECO
Delft, The Netherlands

1986 MARTINUS NIJHOFF PUBLISHERS

a member of the KLUWER ACADEMIC PUBLISHERS GROUP
DORDRECHT / BOSTON / LANCASTER

Distributors

for the United States and Canada: Kluwer Academic Publishers, 190 Old Derby Street, Hingham, MA 02043, USA

for the UK and Ireland: Kluwer Academic Publishers, ~~MTP Press~~ Limited, Falcon House, Queen Square, Lancaster LA1 1RN, UK

for all other countries: Kluwer Academic Publishers Group, Distribution Center, P.O. Box 322, 3300 AH Dordrecht, The Netherlands

Library of Congress Cataloging in Publication Data

ISBN 90-247-3347-2 (hardback)

Copyright

© 1986 by Martinus Nijhoff Publishers, Dordrecht.

All rights reserved. No part of this publication may be reproduced, stored in a retrieval system, or transmitted in any form or by any means, mechanical, photocopying, recording, or otherwise, without the prior written permission of the publishers,

Martinus Nijhoff Publishers, P.O. Box 163, 3300 AD Dordrecht,
The Netherlands.

PRINTED IN THE NETHERLANDS

Preface

Designing and manufacturing structures of all kinds in an economic and a safe way is not possible without doing experimental stress analysis. The modernity of structures, with their higher reliability demands, as well as today's more stringent safety rules and extreme environmental conditions necessitate the improvement of the measuring technique and the introduction of new ones.

Although theoretical/mathematical analysis is improving enormously, an example of which is the finite element model, it cannot replace experimental analysis and vice versa. Moreover, the mathematical analysis needs more and more accurate parameter data which in turn need improved experimental investigations. No one can do all those investigations on his own. Exchange of knowledge and experience in experimental stress analysis is a necessity, a thing acknowledged by every research worker. Therefore, the objective of the Permanent Committee for Stress Analysis (PCSA) is to promote the organization of conferences with the purpose disseminating new research and new measuring techniques as well as improvements in existing techniques, and furthermore, to promote the exchange of experiences of practical applications with techniques. This VIIIth International Conference on Experimental Stress Analysis on behalf of the PCSA is one in a series which started in 1959 at Delft (NL), and was followed by conferences at Paris (F), Berlin-W, Cambridge (UK), Udine (I), Munich (FRG) and Haifa (Isr.). Such a Conference will be held in Europe every fourth year, half-way between the IUTAM Congresses. Close co-operation exists between PCSA on the one hand and the Gemeinschaft für Experimentelle Spannungsanalyse (GESA) of the VDI/VDE Gesellschaft Mess- und Regelungstechnik (FRG) and with the Society of Experimental Mechanics (SEM) on the other.

In this book the papers have been collected that will be discussed at the VIIIth Conference on Experimental Stress Analysis.

The topic of the Conference is "Current Developments and Perspectives in Experimental Mechanics". The PCSA expresses its thanks to the authors who took the trouble to forward papers comprising their experiences in the field of experimental mechanics and hopes that these contributions will fulfill your expectations and help you in solving your stress analysis problems. Moreover, PCSA expects the Conference to contribute to the development and deepening of personal contacts between the participants from all over the world.

It also likes to express its thanks to the Paper Selection Committee members for their evaluation of the papers presented and for their advice and support in drafting the programme. Acknowledgement of thanks is also expressed to the Netherlands Organization for Applied Scientific Research (TNO) and in particular to the fellow-workers of the TNO Corporate Communication Department and those of TNO-IWECO; Institute of Mechanical Engineering. Without their efforts this Conference would not have been possible.

May 1986

H. Wieringa

Chairman Permanent Committee
for Stress Analysis

VI

Organizing Committee

H. Wieringa, Chairman
H. van den Berg, Secretary

Permanent Committee for Stress Analysis

H. Wieringa (The Netherlands)-Chairman
S.I. Andersen (Denmark)
V. Askegaard (Denmark)
M.C. Azevedo (Portugal)
A. Berkovits (Israel)
A.A. Betser (Israel)
R. Bourgois (Belgium)
A. Bray (Italy)
R. Fidler (United Kingdom)
K. Fristedt (Sweden)
J.J. Geerlings (The Netherlands)
M. Gibstein (Norway)
K.H. Laermann (Federal Republic of Germany)
A. Lagarde (France)
A.R.G. Lamas (Portugal)
A. Martin (France)
Chr. Rohrbach (Federal Republic of Germany)
W. Schumann (Switzerland)
P. Stanley (United Kingdom)
D.S. Theocaris (Greece)
M.E. Tschinke (Italy)

Paper Selection Committee for the VIIIth International Conference on Experimental Stress Analysis

H. Wieringa, Chairman (The Netherlands)
K.H. Laermann (Federal Republic of Germany)
P. Stanley (United Kingdom)
J.J.P. Geerlings (The Netherlands)
A.U. de Koning (The Netherlands)

Scientific Secretariat / Editor

H. Wieringa
TNO-IWECO
P.O. Box 29
2600 AA Delft
The Netherlands
Phone: +31/15 608608
Telex: 38192 iweco nl

TABLE OF CONTENTS

**ORIGINAL PAGE IS
OF POOR QUALITY**

Preface	V
1. L. Ben Aicha, Y. Gilibert, and A. Rigolot Measure and Design of Stresses in Adhesive Bonded Trusses: Extensometrical and Laser-Elasticimetrical Methods	1
2. V. Cervenka and P. Bouska Automated Testing of Concrete Compressive Properties	11
3. M. Cousin and J.F. Jullien Metallic Structures Under Mechanical and Cyclical Thermal Loading	21
4. S.S. Issa Response of Spherical Shells Under Apex Load to Varying Proportions	31
5. D.R. Mocanu, N. Ionescu, and E. Spirea Study of Stress Distribution in the Walls of Vessel Containers for High - Pressure Gas	41
6. V. Radianov The Experimental Analysis of the Stress Distribution in a 1000m ³ Spherical Steel Tank from the Petro-Chemical Industry	49
7. R.C. Barros Small-Scale Testing of End-Restrained Tubular Beam-Columns	57
8. T. Jávör and J. Trenčina Experimental Stress Analysis with Automation of Measurements and Data Processing Using Vibro-Wire Gauges During the Construction of One Segmental Box-Girder Prestressed Concrete Bridge	65
9. J.S.W. Taylor An Experimental Investigation of the Behaviour of Flat Rectangular Plates Under the Action of Combined In-Plane and Lateral Loading	75
10. R.H. Scott and P.A.T. Gill Techniques in Experimental Stress Analysis for Reinforced Concrete Structures	87
11. G.T.M. Janssen and J.M.J. Oostvogels Experimental and Theoretical Research into the Collision Resistance of Inland LPG-Carriers	97
12. P. Macura Experimental Stress Analysis at Plastic Deformations	107

VIII

13.	V. Medved Micro-Computer Based Measurement and Processing Method for Human Locomotor System's Take-Off Properties Evaluation	117
14.	N. Waeckel, J.F. Jullien, and A. Kabore Buckling of Axially Compressed Imperfect Cylinders and Ring Stiffened Cylinders Under External Pressure	123
15.	I.M. Allison Stress Analysis of Threaded Connections Secured by Locknuts	133
16.	G.W.M. Peters, A.A.H.J. Sauren, and H.v. Mameren Redesign and Development of a Force Transducer of the Buckle Type	141
17.	A. Causse and J.L. Trolle Determination on Forces and Moments in Pipe Cross-Sections: Fitting of Experimental Strain Measurements on a Mechanical Analytical Model	151
18.	H. Marwitz and J. Stecher Pressure Measurements on Spatially Curved Elastic Surfaces During Crash Tests	157
19.	P. Tegelaar Investigation into the Loosening of Risers in Carbon-Dioxide Cylinders for Fixed Fire-Extinguishing Systems Aboard Ships	165
20.	J. Javornicky Interaction of Stress Concentrations at Pores in a Material Performed by Photoelastic Modelling	175
21.	A. de Kraker and M.J.L. Stakenborg Cepstrum Analysis as a Useful Supplement to Spectrum Analysis for Gear-Box Monitoring	181
22.	D. Rutkowska New Method for Measurement of Time Characteristics of Mechanical Systems	191
23.	A. Lingener and G. Schmidt Automatic Display of Campbell Diagrams of Start-Up and Run-Down Processes	197
24.	W.P. de Wilde and H. Sol Determination of Material Constants Using Experimental Free Vibration Analysis on Anisotropic Plates	207
25.	G.W. Eggeman Biaxial Failure Testing of a Transverse Isotropic Brittle Material	215
26.	W.N. Sharpe, Jr. A System for Crack-Opening-Displacement Measurement and Photomicrography of Cracks at High Temperatures	221

27.	S.E. Swartz and S.T. Yap Evaluation of Recently Proposed Recommendations for the Determination of Fracture Parameters for Concrete in Bending	233
28.	A. Shukla and R. Chona Determination of Dynamic Mode I and Mode II Fracture Mechanics Parameters from Photoelastic Data	245
29.	V. Weissberg and M. Arcan Mode II and Mode III Fracture Testing of Adhesive Joints Using a Stiff Adherend Specimen	255
30.	H.J. Howland An Integrated Software/Hardware Approach to Experimental Stress Analysis	263
31.	H. Kopecki and J. Smykla Experimental-Numerical Hybrid Technique for Stress Analysis of Plates with Holes in Post Buckling State	271
32.	A. Pietrzyk Digital Image Processing in Experimental Mechanics	281
33.	D.M. Stefanescu Comparative Study of the Sensitivity of Various Measurement Techniques on "Glasses"-Shaped Elastic Element Models Analysed by the Finite Element Method	291
34.	A. Asundi and M.T. Cheung Vibration Analysis Using Moire Interferometry	301
35.	C.A. Walker, P. MacKenzie, and J. McKelvie Heterodyne Moire Interferometry - Some Experience of the Development of a Rapid Measurement System	307
36.	J. McKelvie On the Limits to the Information Obtainable from a Moire Fringe Pattern	315
37.	R. Ritter and M. Hahne Interpretation of Moiré Effect for Curvature Measurement of Shells	331
38.	F. Bremand and A. Lagarde Optical Method of Strain Measurement. Application to Study of Circular Bending of a Beam in the Large Strain Range	341
39.	K. Andresen and R. Ritter The Phase Shift Method Applied to Reflection Moiré Pattern	351
40.	C.A. Sciammarella and M.A. Ahmadshahi Detection of Fringe Pattern Information Using a Computer Based Method	359

X

41.	G. Nicoletto Fatigue Life Prediction of Spot-Welded Lap Joints by Moire Interferometry	369
42.	G.H. Kaufmann, A.M. Lopercolo, S. Idelsohn, and E. Barbero Evaluation of Finite Element Calculations in a Curve-Fronted Crack by Coherent Optics Techniques	379
43.	F. Ginesu and C. Pappalettere Real-Time Moire-Holographic Analysis of Plates with Sharp V-Notches in Tension	387
44.	F.M. Furgiuele, M.L. Luchi, and A. Poggialini Investigation on Crack Closure by Real-Time Holo-Interferometry	397
45.	H.P. Rossmanith, R.E. Knaemmler, and A. Shukla Experimental Investigation of Dynamic Contact Problems by Means of the Method of Caustics	407
46.	A.A. Sukere Photometric Methods of Caustics	417
47.	V. Dolhof Evaluation of Strain Gauge Measurements in Elasto-Plastic Area	429
48.	C.C. Hiel Errors Associated with the Use of Strain Gages on Composite Materials	439
49.	M. Kreuzer How to Avoid Errors Caused by Heat Effects in Strain Gage Measurements when Using Scanning Units	447
50.	W.J. Versnel Compensation of Leadwire Effects with Resistive Straingauges in Multi-Channel Strain Gauge Instrumentation	455
51.	D.E. Oliver, W.R.S. Webber, G. Joseph, and J. Gilby Recent Development of the Spate Technique for Measuring Stress in Structures Loaded with Complex Waveforms	465
52.	P. Stanley and W.K. Chan A New Experimental Stress Analysis Technique of Wide Application	479
53.	N. Harwood and W.M. Cummings Use of the Thermoelastic Technique in Experimental Stress Analysis	489
54.	W. Kizler Opportunities and Limitations of Thermoelastic Stress Analysis	499
55.	J. McKelvie Some Practical Limits to the Applicability of the Thermo-Elastic Effect	507

56.	A.S. Redner Pressure-Sensitive Photoelastic Sheets	519
57.	H. Marwitz, W. Kizler, and K. Enslin The Boundary Element Method, an Accelerating Calculation Process Used in Experimental Stress Analysis	525
58.	F.W. Hecker and B. Morche Computer-Aided Measurement of Relative Retardations in Plane Photoelasticity	535
59.	F. Thamm and L. Borbás Checking the Shear-Difference Method in Case of Photoelastic Coating	543
60.	K.-H. Laermann On a Nonlinear Theory of Photoelasticity	551
61.	H.A. Gomide and C.P. Bürger Strain Distribution During Hot Rolling of Strip by Photoelastic Simulation	559
62.	T. Plitt, H. Weber, A. Geissler, and K.-F. Ziegahn On Vibration and Shock Isolation of Sensitive Goods by Viscoelastic Packaging Materials	569
63.	P. Hofstötter Laboratory Tests on Encapsulated High Temperature Strain Gages SG 425 for Measurements up to 530°C	579
64.	C. Amberg Strain Measurements at Variable Temperatures up to 300°C within a Prestressed Concrete Pressure Vessel by Means of Encapsulated Welded Strain Gages	589
65.	Z. Kleczek, A. Zorychta, A. Szuminski, A. Luczak, and Z. Twulski Loss of Stability of Underground Excavations - View on a Possibility of Prediction	599
66.	H.N. Teodorescu, D. Cristea, E. Sofron, and M. Popa Specific Techniques in 2D Stress Analysis	605
67.	A. Strozzi Experimental Stress-Strain Field in Elastomeric O-Ring Seals	613
68.	S. Keil and K. Schäfer Measurement of Tectonic Rock Strain in Iceland	623

MEASURE AND DESIGN OF STRESSES IN ADHESIVE BONDED TRUSSES : EXTENSOMETRICAL AND LASER-ELASTICIMETRICAL METHODS

L. BEN AICHA*, Y. GILIBERT**, A. RIGOLOT***

E.N.S.T.A. - L.M.E.

Groupe Composites et Collage

Centre de l'Yvette, Chemin de la Hunière

91120 PALAISEAU

1. INTRODUCTION

Used since the remotest antiquity, the bonded assemblage has been developed in the technological field since the beginning of the 20th century.

However, the fundamental researches about this way of bonding dates back to, at the very most, forty years. Coupled with important progresses in joint design and improved knowledge of bonding processes, the result is an ever growing variety of adhesive bonded assemblages, depicted for instance in references [1].

One of the aims of this paper is to show with the help of examples, that the extensometrical method with electrical gauges is suitable for the study of the mechanical behaviour of bonded structures.

This method, elaborated by GILIBERT [2] in the years 1971-73, allowed to validate a finite elements method [5].

In 1977-78, GILIBERT and RIGOLOT have developed an analytical theory of double lap bonded joints by using the method of matched asymptotic expansions [3] [4]; since then, the comparison between measurements and computations allowed conclusive progress with regard to this complex domain of solid mechanics.

In 1985, with the collaboration of FERRE [6], BEN AICHA and GILIBERT used a laser-photoelasticity method to measure the stresses in double lap bonded joints with the aim of confirming theoretical results.

2. PREPARATION OF THE SURFACE AND MEASUREMENT OF THE GEOMETRY

2.1. Properties of the Adherends

A low carbon steel (0.18 % carbon; XC 18 French standard equivalent to SAE-AISI 1017) was used for the adherends of the specimens studied. The properties of the steel were controlled using mechanical measurements and microscopic observations. The Young's modulus ($E_T = 207\,700$ MPa) and the Poisson's ratio were determined using tension test with strain gauges at a very low strain rate ($\dot{\epsilon}$ about 10^{-6} s $^{-1}$) on steel specimens with 100 mm 2 square cross section and 250 mm length. The Brinnell hardness (HB = 210) test showed the uniform quality of the material, whereas microscopic observations indicated a ferritic microstructure.

*Thésard ENSTA/LME/GCC

**Chef du Groupe Composites et Collage, Maître de Conférences,
Docteur ès Sciences

***Conseiller Scientifique du G.C.C., Professeur des Universités à Reims

2.2. Preparation of the Rough Adherends, Finishing and Blasting

A shaping machine with a traversing tool was used in the preparation of the rough adherends.

This was followed by milling and after which a grinding was effected with a horizontal surface grinding machine under different conditions : coarse or fine grain grinding wheels. For all these operations, machining conditions (speed, feed, depth of cut, lubrication, sharpening of the tools) were strictly controlled and are described in Reference 2, Chapter 4

The finishing procedure for some of the specimens was completed with sand blasting under four conditions using different particle diameters (115, 169, 282 and 423 μm) or with shot blasting. The particles with a 115 μm diameter were made of high purity white alumina ($\text{Al}_2\text{O}_3 > 99.5\%$), whereas the particles with diameters of 423, 282 and 169 μm were of brown corundum, i.e. less pure alumina (composition : $\text{Al}_2\text{O}_3 > 94\%$; $\text{TiO}_2 < 2.5\%$; $\text{SiO}_2 < .5\%$). The blasting pressure used was 0.4 to 0.5 MPa. The sand jet was inclined at 60° from the specimen surface and displaced at a speed of 24 mm s^{-1} . The shot blasting was conducted with iron shots 1 mm in diameter.

In this paper, the various surface states are designated as follows :

RF - fine ground state ; RFS - fine ground sand blasted state ;

RG - coarse ground state ; RGS - coarse ground sand blasted state ;

RGG - coarse ground shot blasted state.

The numbers following RFS and RGS designate the particle mesh size.

2.3. Measurement of the Surface Roughness Parameters

The surface profiles were determined using probes with an air bearing of 25 μm and 750 μm travel distances. The specimens used had the same section as the adherends and were machined and treated at the same time under the same conditions. The surface profiles were measured, before and after blasting, along reference paths, the ends of which are marked with two notches remaining after blasting.

Data were recorded and processed by a computer to determine the various parameters of the surface defects describing the total profile, roughness and waviness. The calculations were done using a method developed by B. Scheffer of RENAULT (FRANCE).

We observed that the surface roughness parameters alter very quickly during the first few seconds of blasting and do not change after a while. We selected a time lapse of 30 seconds which ensured a stable state of these parameters.

Measurements showed that the surface roughness parameters are not dependent on the direction of measurement for blasted states, whereas condition as ground showed some anisotropy.

Reference 2, chapter IV, table IV.1 presents values of the surface roughness parameters for the various surface states studied. These are the total depth of roughness, R_t ; the average depth of roughness, R ; the maximum depth of roughness, R_{max} ; the roughness levelling depth, R_p ; the arithmetical mean deviation from mean line of roughness, R_a ; and average spacing of roughness, R_p .

From these data, it can be seen that the surface roughness parameters for sand blasted states depend on both the initial grinding and the mean diameter of the particles used for blasting. For all surface preparations, the maximum depth of roughness R_{max} is very close to the total depth R_t , which indicates that surfaces have no aberrant defects of roughness and are consequently fairly homogeneous ; for the fine ground state, the roughness parameters increase steadily with the particle diameter whereas for

the coarse ground state these increase notably only for a diameter superior to 200 μm .

Other surface defect parameters were computed but proved of little importance as far as the mechanical properties of the joints are concerned. However, they confirmed that the prepared surfaces had well defined and reproducible parameters.

2.4. Properties of the adhesive

We used the commercial adhesive, Eponal 317, of Sonal, France, which is a two component system (an epoxy resin containing mineral fillers and a hardening agent). It was processed at room temperature ; at such temperature, about 20 minutes are available for use and polymerization rate reaches 90 % within 2 hours.

We determined its mechanical, physical, structural and chemical properties. The elastic constants were measured at room temperature (20°C) using two methods. Tensile test using strain gauges and a very slow loading rate ($\dot{\epsilon}$ about 10^{-6} s^{-1}) showed an elastic brittle behavior. Using traction test the Young's modulus was found to be 5800 MPa, the Poisson's ratio was 0.327 and the strength was 30 MPa ; whereas ultrasonic measurements gave 5940 MPa for the Young's modulus and 0.323 for the Poisson's ratio. The measured density was 1.433 kg dm^{-3} .

3. DESIGN AND MANUFACTURE OF THE TEST-SPECIMENS-LOADING CONDITIONS

We used specimens with two double-lap joints. One of these double-lap joints was used for strain measurements. The other joint, which was tightened transversely by a binding clip, ensured axial and uniform load in the adherends, while the clip eliminated any local bending. The extremities of the test-specimen were fixed on a universal testing machine by knee joints. In fact, this design of the specimen ensured symmetrical fractures in the tested part, and the clip decreased considerably the statistical deviation in the measurements, as shown in Reference 2, Chapter 2. Figure 1 shows a schematic view of the specimen.

The parts (10 mm x 4.5 mm cross-section for parts 2' ; 10 mm cross-section for parts 1') were produced at a $\pm 0.01 \text{ mm}$ tolerance. The length of the overlap in the tested part of the specimen was 88 mm. A thickness of 0.5 mm was selected for the adhesive joint and controlled by gauged spacers. Preliminary tests, described in Reference 2, Chapter 11, showed that this thickness gives the best mechanical behavior for these dimensions of the metallic parts and this length of the joint. The test-specimens were loaded in tension at a slow rate (1000 N per minute) at room temperature (20°C).

4. PRINCIPLE OF THE MECHANICAL MEASUREMENTS

Since mechanical quantities inside the joint cannot be obtained directly, we used electric strain-gauges placed at different points on external surfaces of the metallic adherends. Figure 1 shows the position of the gauges ; their distances from the middle of the joint are as follows :

- gauge 1 : + 37 mm
- gauge 2 : - 18.5 mm
- gauge 3 : 0
- gauge 4 : + 18.5 mm
- gauge 5 : + 37 mm

The positioning of the gauges is described in detail in Reference 2, (Chapter 5).

A sensitive and precise ($\pm 0.25\%$) bridge (VE 20 Micromasurement) was used.

Figure 2 shows typical strain gauge recordings for a ground sand blasted state. Other recordings are given in Reference 2.

Principle of the mechanical Measurements is described by references 2 and 7

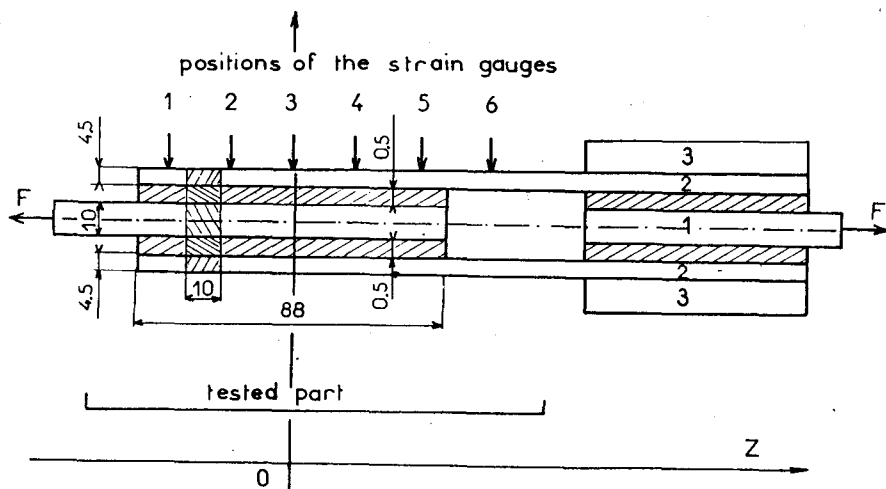


Figure 1. Schematic view of the test-specimen (dimensions in mm). A view of the cross-section is superimposed between gauges 1 and 2. 1' and 2' : adherends ; 3' : binding clip.

Visual and microscopic observations of the fractured specimens have confirmed that in the central part of the joint a progressive shear fracture occurs inside the adhesive ; at the ends of the joint one can see either a shear fracture inside the adhesive or an adhesive failure between the adhesive and the metallic adherend along the upper or lower face, induced during the final phase of the fracture.

These facts differentiate the ground sand blasted state from the ground state, which showed predominantly metal-resin adhesive fractures.

The various stages for the ground sand blasted states, (i) elastic behavior, (ii) initiation of micro-cracks, (iii) coalescence of the micro-cracks, (iv) stable propagation of the cracks, and finally, (v) unstable propagation up to final fracture, proved to be absolutely reproducible (Reference 2, Chapter 8).

These experimental results can be partly explained by the various theoretical analyses [3, 4, 8], which have analyzed stress fields in adhesive joints. However, these theoretical analyses, which are based on continuum mechanics and use idealization of interfaces, cannot explain the significant differences observed using the above measurement procedure, and are presented below.

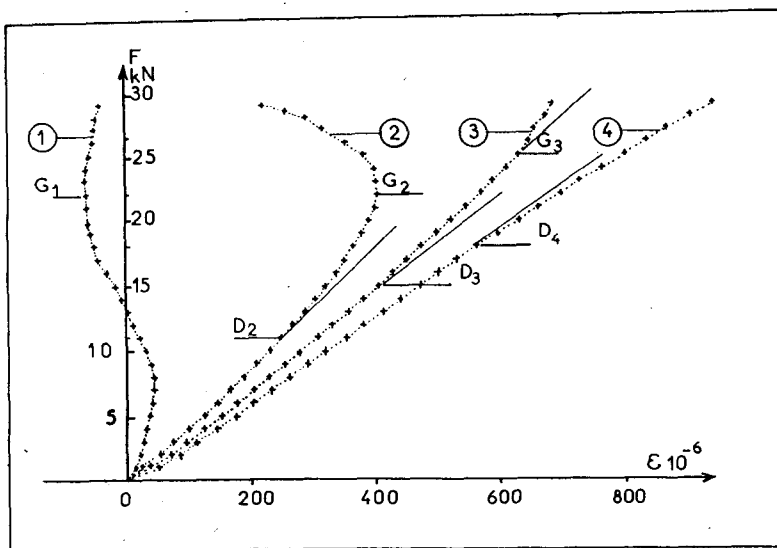


Figure 2. Strain versus tensile load for a ground sans blasted state (outputs of gauges 1-4). Non-linearity occurs over point D_2 .

5. EFFECTS OF ROUGHNESS ON MECHANICAL RESULTS

Here are presented the effects of roughness on the three typical mechanical parameters : elastic limit (crack initiation threshold), crack propagation threshold, and ultimate strength.

We found that roughness can be adequately represented by using the total depth of roughness R_t .

We observed a very small scattering in the measured values, which gives proof of the importance of our careful and well-defined process in preparation and testing. Deviation in the results is generally higher for the propagation threshold and the ultimate strength than for the elastic limit. Further, deviation in the ultimate strength is higher for non-blasted surfaces than for blasted surfaces (Reference , Chapter 8). Typical values, corresponding to the results presented in Figure 3, are (i) 0.25 kN for the crack initiation threshold (about 12 kN), (ii) 0.5 kN for the crack propagation threshold (about 24 kN), and (iii) 0.5 kN for the ultimate strength (about 30 kN).

For the sand blasted states, we found that the mechanical parameters were influenced by the initial grinding and the roughness, which is related to the sand particle size.

The fine grinding is equivalent or better than the coarse grinding for the three mechanical parameters ; it gave better values for the elastic limit with all diameters.

For both types of grinding, we observed that the strain measurements given by the gauges at the external surface of the adherends were significantly smaller (for any position) and more uniform along the specimen, when the surfaces were prepared using particles with a diameter of 169 μm . Further-

more, this preparation shows the best values for the three mechanical parameters.

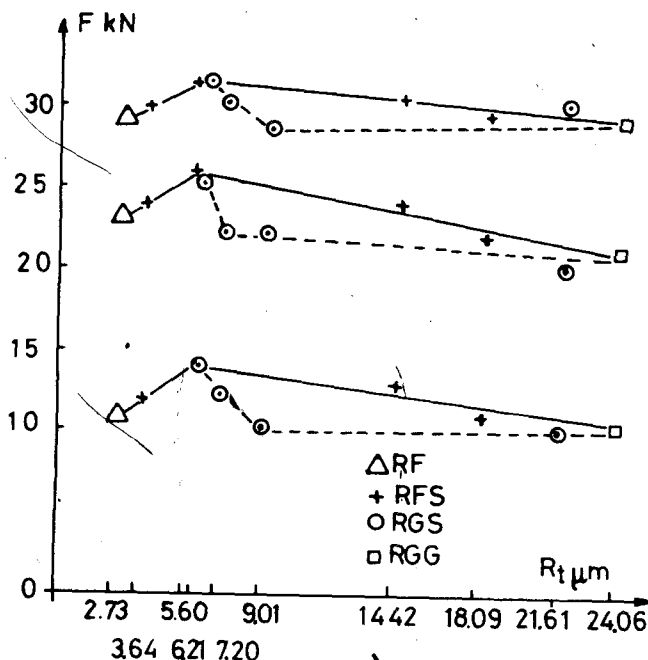


Figure 3. Mechanical parameters versus the total depth of roughness : from the bottom, (i) crack initiation threshold, (ii) crack propagation threshold, and (iii) ultimate strength. For fine grinding without blasting (RF) the values are in accordance with the extrapolation (with respect to the roughness) of those obtained for fine grinding with blasting (RFS).

Figure 3 summarizes the results. Almost all of the plotted points represent the mean value of four tests. In Reference 2, Chapter 9, one can find the curves representing F versus the other roughness parameters, R_a , R_p , R ; they have the same behavior as the curves in Figure 6.

Figure 3 shows that for fine grinding, with or without blasting, the three mechanical parameters reach a maximum value when the total depth of roughness equals $5.6 \mu\text{m}$. It seems possible to associate this property with the fact that the total depth of roughness is approximately the size of the fillers in the resin.

No precise trends can be found in the case of coarse grinding.

6. COMPARISON BETWEEN THEORETICAL AND EXPERIMENTAL RESULTS

For an optimal state ($e_f = 0.5 \text{ mm}$), we see on figure 4 a good correlation in the elastic domain between theoretical results [3] [4] [8] and experimental measures. Some difference appears in the neighbourhood of the free end of the upper adherend : it was impossible to introduce in computations the effects of the angular singularities in these regions.

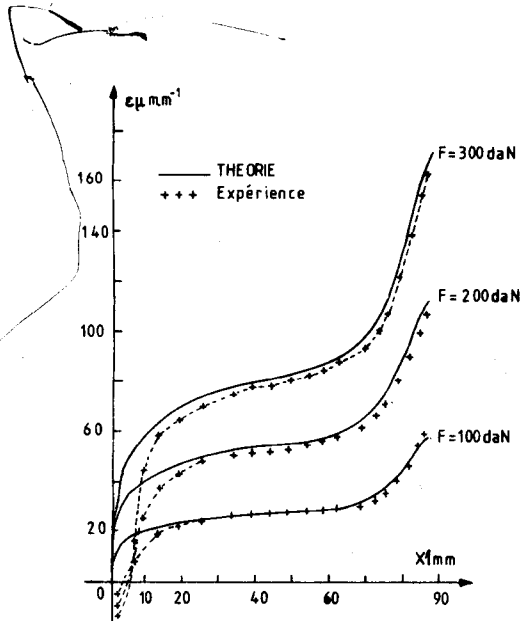


Figure 4. Longitudinal deformations versus distance of the measurement. Localization from the free ends of the adherends (T_1 and T_2 , figure 5)

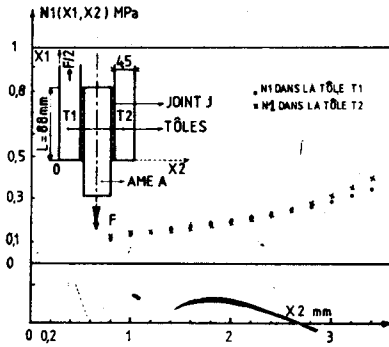


Figure 5. Principal stresses in adherends T_1 and T_2 at abscissa $X_1 = 10,5$ mm versus the thickness coordinate X_2 .

7. STRESS MEASUREMENTS BY A LASER PHOTOELASTICIMETRICAL METHOD

The truss is made in the same way that the one depicted in Figure 1, whose adherends in polycarbonate (PSM-1) are joined by PC1 adhesive (Vishay Micro-mesures, Young's modulus : $E_{PSM.1} = 2400$ MPa ; $E_{PC1} = 3150$ MPa. POISSON'S ratio : $\nu_{PSM.1} = 0.38$; $\nu_{PC1} = 0.36$; Figure 5.)

Principal stresses, measured by an automatic laser-photoelasticimeter, are presented in Figure 6. It's to be noted that the shape of the curve in figure 6 is similar to the experimental one depicted in figure 4, especially in the neighbourhood of the free edge of the adherend.